Design and Development of Defected Ground Structure Fractal Antenna based on Osgood Curve for C-band Modern Wireless Communications

Gurmeet Singh[1], Ashish Kumar[2]

[1]School of Computing Science and Engineering, Galgotias University, Greater Noida, India
[2]Chitkara University Institute of Engineering and Technology, Chitkara University, Punjab, India

Corresponding author: Ashish Kumar (e-mail: ashish.1130@chitkara.edu.in)
Co Corresponding author: Gurmeet Singh(e-mail:gurmeet.singh@galgotiasuniversity.edu.in)

ABSTRACT Multifunctional behavioral antennas are one of the significant features of the modern wireless communication systems. This is due to the fact that the miniaturized sizes of the devices demand compact and low-profile antennas that cover limited space and provide multi-frequency functionalities over a wide range of the spectrum. In view of these prerequisites, this paper presents the two design approaches utilizing Osgood Curve Fractal structure as the antenna element with different feeding techniques. The proposed antennas resonate at multiple frequencies covering S- and C-band with excellent impedance matching. The designs have been optimized in terms of scaling factor and position of microstrip feed line with peak gain of 4.5 dBi. Design 1 has significant bandwidth for required applications; however, design 2 possesses low bandwidth with small frequency ratio. Both the proposed designs are fabricated, and results are quite promising. The proposed designs can be utilized for various sub-6 GHz 5G automotive applications as it can easily integrated in the various parts of the modern passenger car.

INDEX TERMS Automotive Applications, Bandwidth, Fractal, Optimization, Osgood

I. INTRODUCTION

IN today's era of modern wireless communication including 5G/6G new radio (NR) features, high data rate, reliable connection and multifunctional element are of the significant features of any wireless device [1-2]. Therefore, multiband antennas are to be considered a key component for achieving these characteristics and there are different ways available in the literate to achieve the multiband property of the antenna elements [3]. These methods include slotted antennas, defected ground structure (DGS), use of meta-material, use of multi-input-multi-output (MIMO) antenna configurations, use of fractal structures etc [4]. Among these methods, fractal geometry would be the most popular method to achieve the multiband characteristics in the antenna [5-6]. There are some of the common fractal geometries that are used by the researchers in the antenna such as Koch fractal, Sierpinski Carpet, Hilbert Curve etc. or hybrid structures [7-9]. For instance, a compact Sierpinski triangle antenna is discussed in [10] for X-band applications. Similarly, a modified Koch fractal antenna is presented for multiband characteristics including C-band and X-band for telemedicine applications. However, a DGS is applied in this design to improve the performance characteristics of the proposed antenna in the required band of frequency. In another research [11], a dual band operation has been performed by adapting the cantor-based fractal geometry antenna. The proposed design finds applications for Bluetooth, WLAN and WiMAX. Similalrly in another article [12], multiband behavior has been observed by considering the novel star-based fractal antenna covering the frequency range from 4.5 GHz to 17 GHz for military communication systems. In [13], a Co-planer waveguide (CPW) fed monopole fractal antenna with hexagonal shape is projected for ultra-wide band (UWB) applications. Again in [14], a slot antenna with seven frequency bands has been presented with a very small frequency ratio. Moreover, this antenna possesses circular polarization to reduce the polarization losses and hence enhance the performance of the antenna. In the recent research presented in [15],a spiral fractal antenna is projected and arranged in MIMO configuration for C-band applications. In the continuation of the same, a compact leaf fractal antenna is presented considering frequency reconfigurability for 5G, LTE applications [16]. In [17], a honeycomb fractal structured antenna is presented for vehicular communications. The projected design operates in the frequency band from 0.85 GHz to 5.9 GHz with peak gain of 7.43 dBi.

From the above literature survey, it is evident that there is much scope in designing and optimizing the compact fractal structure for the sub-6 GHz NR frequency bands. This paper presents the two design approaches for Osgood

curve antenna. The design considerations are presented in section 2. The optimization process is discussed in section 3 and results are outlined in section 4 followed conclusion in section 5.

II. PROPOSED ANTENNA DESIGNS

In this article, a novel fractal geometry named Osgood curve has been adapted for the antenna design. During the design, two different approaches have been discussed for radiator design. Both the antenna configurations have been manufactured upon FR-4 substrate material with thickness = 1.6 mm. In first design, initially a rectangle has been chosen and V-shaped slot is etched at the center along the length of the patch and the same is repeated in each iteration as shown in figure 1. The patch is fed with 50 Ω microstrip line and the overall size of the proposed design is 37.95 mm × 40 mm × 1.6 mm. Further, the position of the feed of the design has been optimized using Whale Optimization Algorithm (WOA). Similarly, in design 2, the fractal iterations have been imposed on both length and width side of the patch as shown in figure 2. This design uses fractal antenna, which is created by splitting the patch's side into four uneven pieces and rearranging them into a Koch curve-like pattern. Similar to the Koch curve but with a faster rate of shrinkage, the Osgood curve is applied to the sides of the patch. The coaxial feeding method is employed to feed this antenna efficiently, and by placing the feed at the ideal spot, perfect impedance matching has been obtained. Probe feed has an outer radius of 2.1 mm and an inner radius of 0.65 mm. The complete size of the design 2 is 40×40×1.6 mm^3. Moreover, the dimensions of the proposed designs are shown in figure 3.

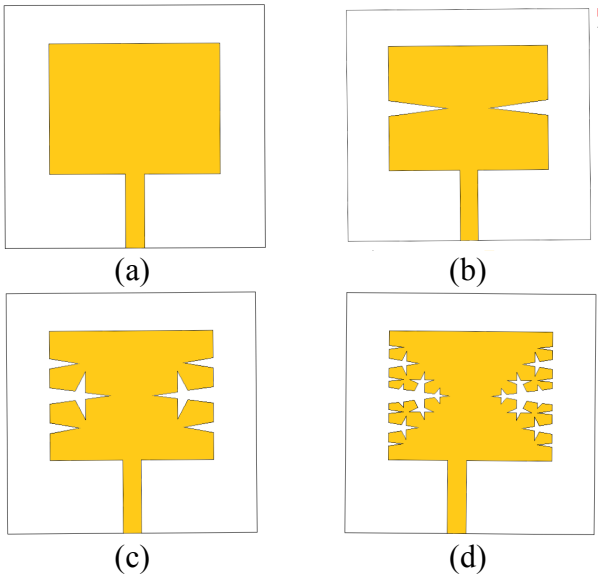

Figure 1. Various Iterations of Design 1 (a) zeroth (b) First (c) Second (d) Third

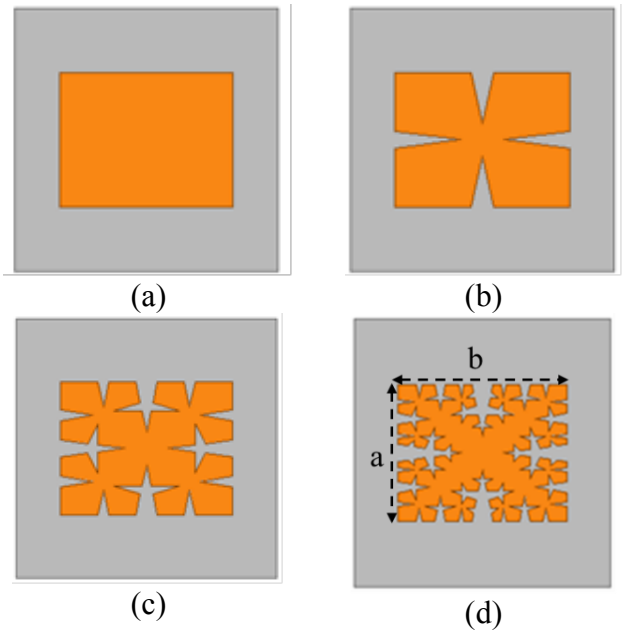

Figure 2. Various Iterations of Design 2 (a) zeroth (b) First (c) Second (d) Third

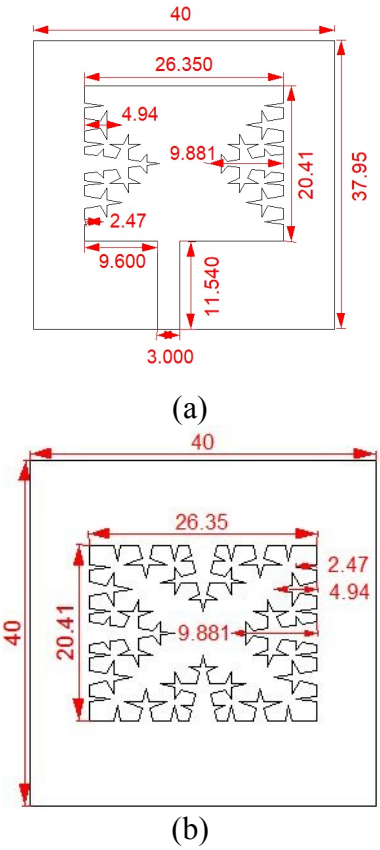

Figure 3. Dimensional considerations of the proposed antennas (a) Design 1 (b) Design 2 (All dimensions in mm)

III. OPTIMIZATION OF THE PROPOSED ANTENNAS

A. Feed Optimization in Design 1

Both the antennas have been optimized in different ways. For instance, in design 1, the position of the microstrip feed has been optimized to achieve the required bandwidth as the bandwidth is significantly impacted by the position of the feed. Therefore, a mathematical relation has been established between these two components using curve fitting technique in MATLAB. Based on the humpback whale's hunting strategy, the Whale Optimization Algorithm uses these polynomial relations to produce the objective function needed to obtain the optimal feed site. WOA essentially carry out three fundamental actions mathematically: searching, encircling, and assaulting. Equations (1), (2), and (3) update the random vector position $\vec{A}$ based on the value of the variable's probability p.

$$\vec{D} = \vec{Z}\vec{Y}^{*}(t) - \vec{Y}(t) \quad (1)$$

$$\vec{Y}(t+1) = Y_{rand} - T.D \quad (2)$$

$$\vec{Y}(t+1) = \vec{D}^{'}e^{bl}.\cos(2\pi l) + \vec{Y}^{*}(t) \quad (3)$$

Where present iteration is represented by t and T, Z and Y* are coefficient and location vector of the optimum solution. $\vec{D} = |\vec{Y}^{*}(t) - Y(t)|$ expresses the spacing amongst ith whale and target, the profile of the logarithmic twisting figure is interpreted by b,*l* characterizes arbitrary number in range [−1,1] [26]. The polynomial relation in equation (4) along with objective function is used in WOA to minimize objective function given below in equation (5).

$$y = -0.3\times x^{3} + 13.3\times x^{2} - 161x + 571 \quad (4)$$

The objective function provided by equation (5) is minimized using WOA by using the relation (4) mentioned above. It was created to determine the precise feed position needed to maximize the fractal antenna's bandwidth and the optimized value is 16.425 mm

$$BW = (79 - y)^{2} \quad (5)$$

B. Scaling Factor Optimization in Design 2

The overall size of design 2 has been scaled by keeping the fixed feed position and fixed dimension b with varying dimension a as shown in figure 2 (d). The corresponding variations can be visualized in figure 4. It can be depicted that for the required frequency bands and impedance matching, a=b=1 has been chosen the best scaling factor

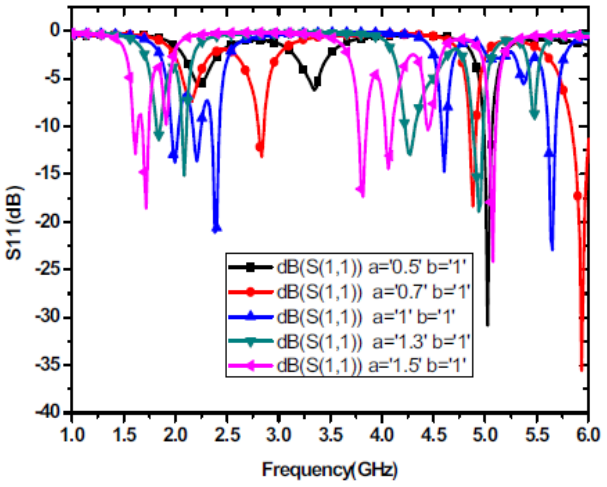

Figure 4. Reflection Coefficient with scaling factor optimization

IV. RESULTS AND DISCUSSIONS

The first parameter to assess the specifications of the proposed antenna is the reflection coefficient. The S_{11}(dB) of all iterations of design 1 with center feed position is shown in figure 5 (a). This graph shows that the antenna's resonance frequency is 5.24 GHz for the zeroth iteration, 6 GHz for the first, 5.68 GHz, 6.46 GHz for the second, and 5.52 GHz, 6.2 GHz for the third. The projected fractal antenna, as shown in figure 5(b), resonates at 5.27,5.6, 5.77, and 6.2 GHz with impedance bandwidth well below -10 dB. The performance parameters of design 1 are illustrated in Table 1. Current distribution of the design at different resonating frequencies is shown in figure 6.

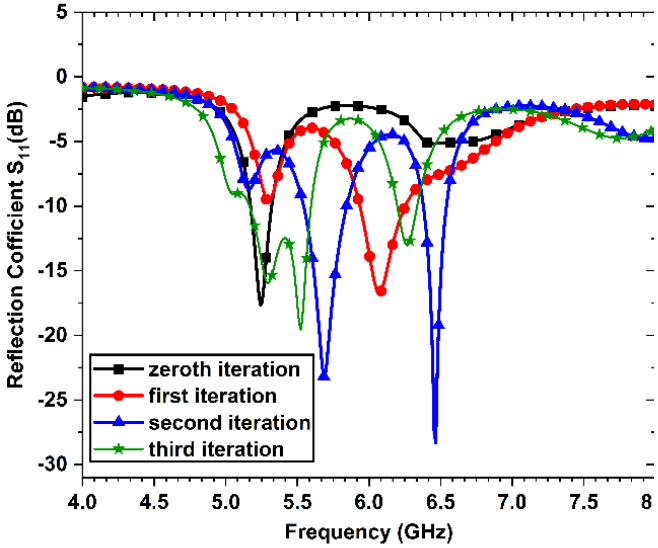

Figure 5. Reflection coefficient of Design 1 (a) Variations with all the iterations

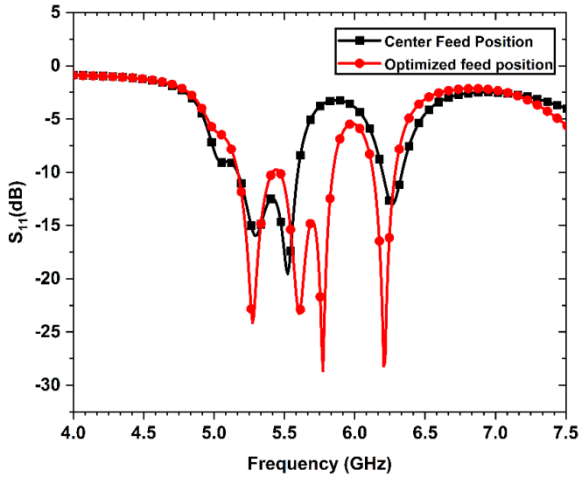

Figure 5. Reflection coefficient of Design 1(b) Effect of feed position optimization on reflection coefficient

TABLE 1. Performance parameters of design 1 with feed position optimization

Design 1 Specifications	Resonant Frequency	S_{11} (dB)	Bandwidth (MHz)
Center feed position	5.52	-19.55	420
	6.26	-13.03	130
Optimized feed position	5.27	-24.15	240
	5.6	-23.2	270
	5.77	-28.68	150
	6.2	-28.23	130

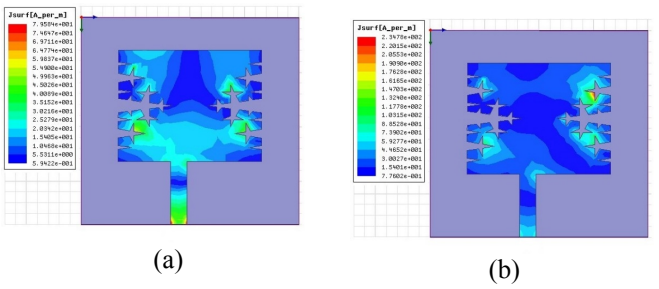

(a) (b)

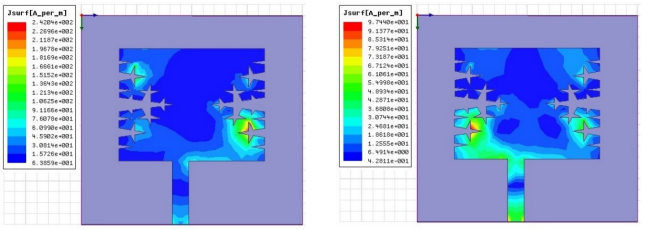

(c) (d)

Figure 6. Current Distribution of Design 1 (a) 5.27 GHz (b) 5.6 GHz (c) 5.77 GHz (d) 6.2 GHz

Further, the reflection coefficients of all the repetitions of design 2 are shown in figure 7. Finite element based high frequency structure simulator used for the assessment of the antenna performance and these performance parameters measured in terms of S_{11}(dB), bandwidth and frequency ratio. Reflection coefficient variations with iterations of design 2 are depicted in figure 6, This demonstrates that the antenna resonates at 2.24 GHz, 2.52 GHz, and 2.94 GHz at the first iteration and 2.66 GHz, 3.32 GHz at the zeroth iteration. Likewise, for the second iteration, the antenna resonates at 2.08 GHz, 2.31 GHz, 2.57 GHz, and 4.83 GHz; for the third iteration, the antenna resonates at five frequencies with a tiny frequency ratio, which are 1.99 GHz, 2.20 GHz, 2.40 GHz, 4.85 GHz, and 5.53 GHz. The performance characteristics of design 2 are illustrated in Table 2. The current distribution of design 2 at the operating frequencies is shown in figure 8.

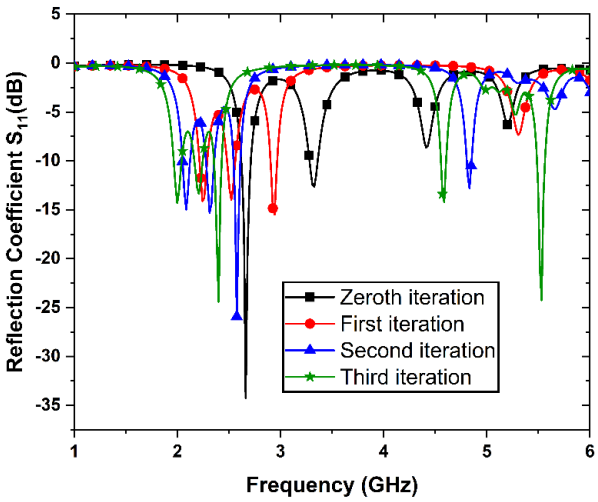

Figure 7. Reflection coefficient variations of Design 2 with all the iterations

TABLE 2. Performance parameters of design 2

Design 2 Specifications	Resonant Frequency	S_{11} (dB)	Bandwidth (MHz)	Frequency Ratio
With Coaxial Feed Optimization	1.99	-13.3	50	1.105
	2.20	-24.4	70	1.09
	2.40	-14.31	50	2.02
	4.85	-14.19	50	1.14
	5.53	-24.23	70	

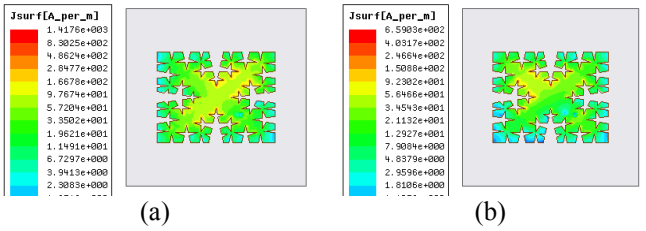

(a) (b)

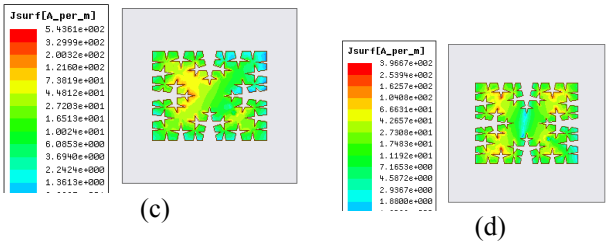

(c) (d)

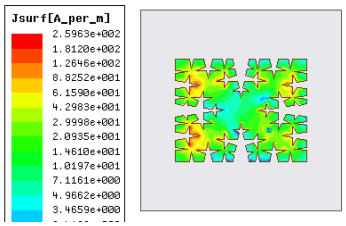

(e)

Figure 8. Current Distribution at (a) 1.99 GHz (b) 2.2 GHz (c) 2.4 GHz (d) 4.58 GHz (e)5.53 GHz

V. FABRICATED AND MEASURED RESULTS

The fabricated prototypes of both designs are shown in figure 9. Figure 9 (a) illustrates the top view of design 1 and figure 9 (b) shows the back side of the design 1 which incorporates the spiral shape defected ground structure. The DGS will improve the overall gain and bandwidth of design 1. In the similar way, figure 9 (c) shows the top view of design 2 which depict the Osgood fractal structure on both length and width side of the patch with coaxial feed at the optimum position to achieve the excellent impedance matching. Further, the reflection coefficient comparison of design 1 is depicted in figure 10, which shows close agreement between simulated and measured reflection coefficient except very minute shifting round 5.27 GHz, and the second peak is observed between the 5.6 GHz and 5.77 GHz as compared to simulated curve but still satisfying the criteria of -10 dB impedance bandwidth in the desired operating band. Finally, a very small shift of a few MHz can be observed around 6.2 GHz with degraded impedance matching but still well below -10 db. In a similar way, reflection coefficient comparison of design 2 is illustrated in figure 11, which shows very close agreement between simulated and measured results except variations in the impedance matching at respective resonating frequencies without shifting in the resonating frequency. This is due to the fact that there are imperfections in the fabrication of coaxial feed, which is fed in very limited space.

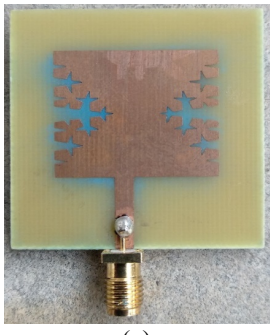

(a)

(b)

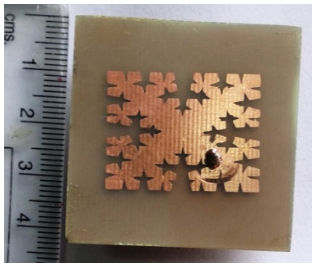

(c)

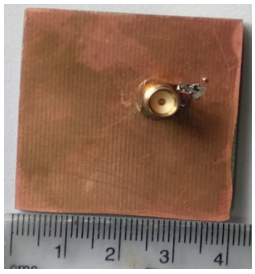

(d)

Figure 9. Fabricated Prototype (a) Design 1 top view (b) Design 1 back view (c) Design 2 top view (d) Design 2 back view

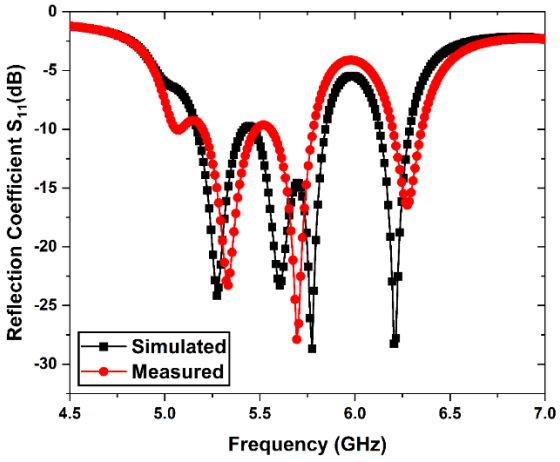

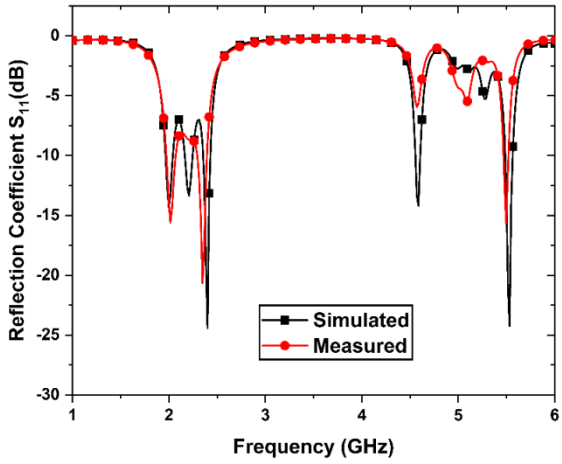

Figure 10. Simulated and Measured Reflection Coefficient of (a) Design 1 (b) Design 2

Next, for far field characteristics, the simulated and measured 2D radiation pattern of design 1 at resonating frequencies is shown in Figure 12. At 5.27 GHz, the nature of the pattern is broadside direction in both the planes (Phi=0° and 90°). However, at Phi=0°, the major lobe pattern is shifted and at Phi=90° the pattern is directed towards the zenith. Similarly, at 5.6 GHz, the nature of broadside direction but with some tilted pattern in opposite directions in both the planes. Further, the patterns are of broadside nature in both the planes directing towards zenith at 5.77 GHz and finally, the pattern shows little side lobe level at Phi=90° and tilted around θ = 30° at Phi = 0° at 6.2

GHz. Overall, there is a close correlation between simulated and measured radiation patterns of design 1 in both the planes at all the resonating frequencies.

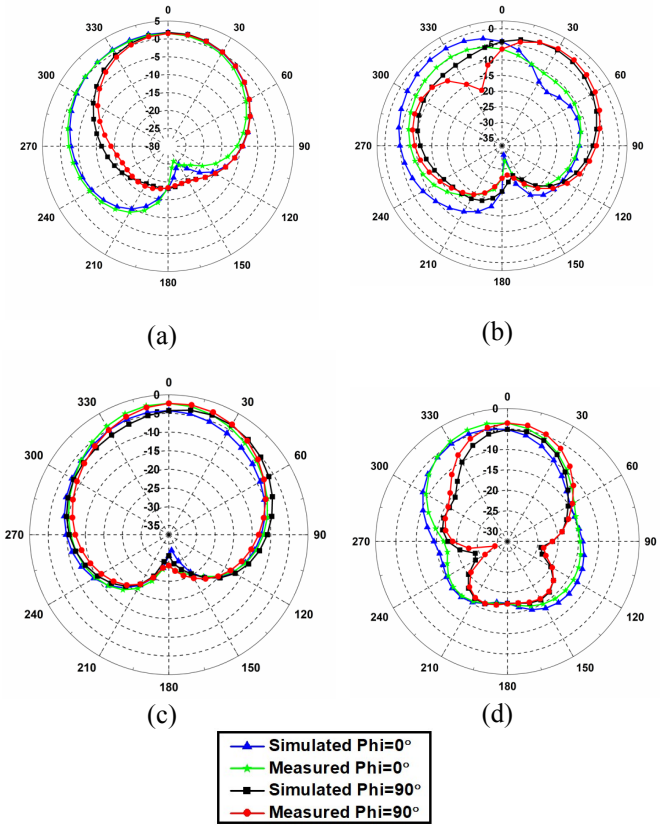

Figure 11. Simulated and Measured Radiation Patterns of Design 1 at (a) 5.27 GHz (b) 5.6 GHz (c) 5.77 GHz (d) 6.2 GHz

Similarly, comparison of the simulated and measured 2D radiation of design 2 is shown in figure 12. The figure describes the nature of the radiation patterns at all the resonating frequencies of design 2. The shape of the patterns at lower frequencies i.e. 1.99, 2.2 and 2.4 GHz is almost similar and the patterns are tilted at Phi=90°. The patterns are in good agreement expect 2.4 GHz. Moreover, the radiation pattern at 4.58 GHz shows two major lobe and null in the broadside direction at Phi=90° with very little interference of pattern at Phi=0°. Finally, the patterns are in broadside direction in both the planes at 5.53 GHz.

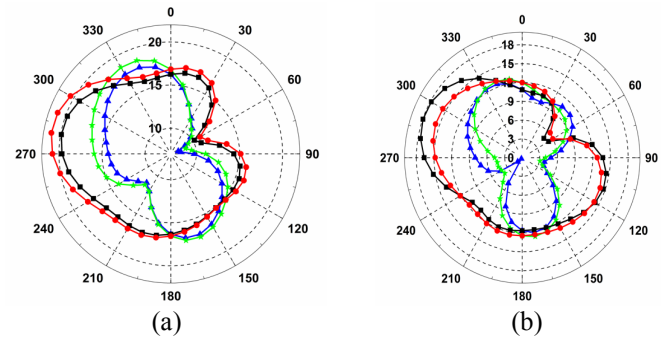

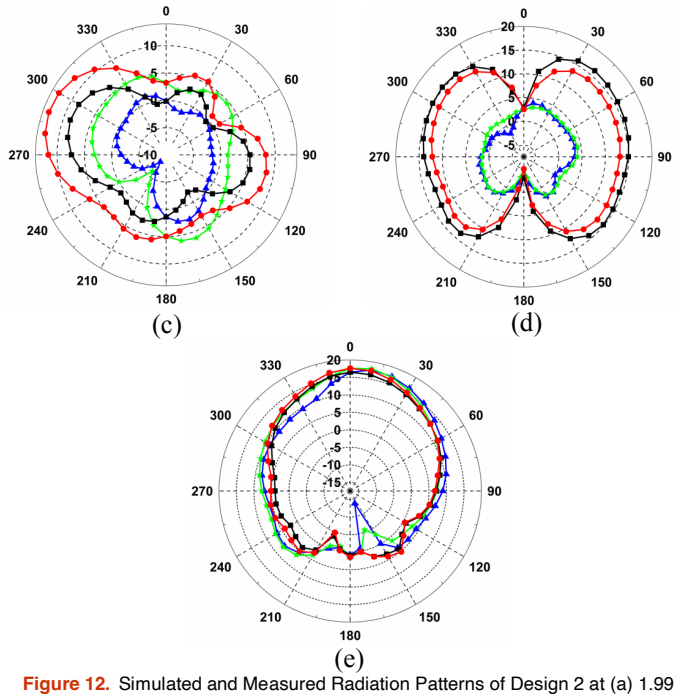

Figure 12. Simulated and Measured Radiation Patterns of Design 2 at (a) 1.99 GHz (b) 2.2 GHz (c) 2.4 GHz (d) 4.58 GHz (e) 5.53 GHz

The proposed antenna design's performance has been compared with other recent similar work in Table 3. In this table other researchers have used the various optimization algorithms like particle swarm optimization (PSO), Dragonfly algorithm (DFO) and Artificial Neural Networks (ANN) to improve the performance parameters. For instance, feed position has been optimized using PSO in [18] to achieve the 4 resonating frequencies, while presented design 2 provides the 5 resonating frequencies in the same band. Similarly, authors in [23] and [24] optimized the height of the substrate and length of the patch using PSO to achieve the required resonating band. Also, the authors of the same paper have optimized the geometrical dimensions of the DGS to achieve the required performance parameters of the intended applications.

TABLE 3. COMPARATIVE ANALYSIS OF THE PROPOSED DESIGN WITH OTHER LITERATURE

References	Size (mm × mm)	Frequency (GHz)	Gain (dB)	BW (GHz)	Optimization Algorithm
[18]	34 × 36	2.45, 5.4, 6.65, 8	8.55	0.31	PSO
[19]	38 × 45	2.05 - 14.5	6.5	18	PSO
[20]	36 × 20	3.3,4.9,6.4,7.7, 8.9,12.37	5.8	0.42	PSO
[21]	20 × 17	5.5 & 6.7	N.A.	8.15%	ANN
[22]	55 × 60	2.6, 4.4 & 8.7	7.3	4.19	DFO
[23]	27.6 × 20.2	3.1-10.6	7.84	9.9	PSO
[24]	30.2 × 20	5.88, 6.70, & 7.23	4.5	1.8	PSO
[25]	30 × 30	1.95, 3.94, 5.25, 7.03	N.A.	0.95	PSO
This Paper	40 × 40	1.99-6.2	4.5	0.27	WOA

VI. Conclusion

This paper presents the two design approaches of the Osgood based fractal antenna for multiband operations. Both designs have been optimized based on scaling factor and feed position to achieve the required performance parameters. Design 1 possesses the Osgood structure slot along its length only and design 2 comprises of the same structure on both length and width side of the patch. The measured results of both the designs have been compared with the simulated ones after fabricating the prototype. Design 1 covers the frequency in C-band which includes 5.27, 5.6, 5.7 and 6.2 GHz with peak gain of 4.5 dBi and design 2 covers both S- and C-band which includes 1.99, 2.2, 2.4, 4.58, 5.53 GHz. The proposed design can be used for various Sub-6 GHz automotive wireless applications.

References

[1] T. Addepalli, M. Sharma, M.S.Kumar, G.N. Kumar, P.R. Kapula and C.M. Kumar,“ Self-isolated miniaturized four-port multiband 5G sub 6 GHz MIMO antenna exclusively for n77/n78 & n79 wireless band applications, Wireless Networks, pp. 1-17, 2023.

[2] M. Sharma, “Design and Analysis of MIMO Antenna with High Isolation and Dual Notched Band Characteristics for Wireless Applications”, Wireless Pers Commun 112, 1587–1599 (2020). https://doi.org/10.1007/s11277-020-07117-4.

[3] M. Sharma et al., "Miniaturized Quad-Port Conformal Multi-Band (QPC-MB) MIMO Antenna for On-Body Wireless Systems in Microwave-Millimeter Bands," in IEEE Access, vol. 11, pp. 105982-105999, 2023.

[4] Ekta Thakur, Naveen Jaglan, Anupma Gupta, and Ahmed Jamal Abdullah Al-Gburi, "Multi-Band Notched Circular Polarized MIMO Antenna for Ultra-Wideband Applications," Progress In Electromagnetics Research M, Vol. 125, 87-95, 2024.

[5] M. Gupta and V. Mathur, “A new printed fractal right angled isosceles triangular monopole antenna for ultra-wideband applications,” Egypt. Informatics J., 2017.

[6] Y. Kim and D. L. Jaggard, “The fractal random array,” Proc. IEEE, vol. 74, no. 9, pp. 1278–1280, 1986.

[7] S. A. Hamzah, M. K. Raimi, N. Abdullah, and M. S. Zainal, “Design, simulation, fabrication and measurement of a 900MHz Koch fractal dipole antenna,” in SCOReD 2006 - Proceedings of 2006 4th Student Conference on Research and Development “Towards Enhancing Research Excellence in the Region,” 2006.

[8] K. J. Vinoy, K. A. Jose, V. K. Varadan, and V. V. Varadan, “Hilbert curve fractal antenna: A small resonant antenna for VHF/UHF applications,” Microw. Opt. Technol. Lett., vol. 29, no. 4, pp. 215–219, May 2001.

[9] Y. K. Choukiker and S. K. Behera, “Microstrip line-fed modified Sierpinki fractal monopole antenna for dual-wideband applications,” in 2010 International Conference on Communication Control And Computing Technologies, 2010, pp. 17–20.

[10] A. Shokyfeh, “Modified Square Fractal Antenna for Multiband Application,” Int. J. Commun. Antenna Propag., vol. 5, no. 5, p. 297, Oct. 2015.

[11] J. Ali et al., “Cantor fractal-based printed slot antenna for dual-band wireless applications,” Int. J. Microw. Wirel. Technol., vol. 8, no. 2, pp. 263–270, Mar. 2016.

[12] N. Rao, A. Malik, R. Kumar, S. Goel, and D. Kumar V, “Novel star-shaped fractal antenna for multiband applications,” Int. J. Microw. Wirel. Technol., pp. 1–7, 2015.

[13] H. Fallahi and Z. Atlasbaf, “Bandwidth enhancement of a CPW-fed monopole antenna with small fractal elements,” AEU - Int. J. Electron. Commun., vol. 69, no. 2, pp. 590–595, Feb. 2015.

[14] P. Chaurasia, B. K. Kanaujia, S. Dwari, and M. K. Khandelwal, “Design and analysis of seven-bands-slot-antenna with small frequency ratio for different wireless applications,” AEU - Int. J. Electron. Commun., vol. 99, pp. 100–109, Feb. 2019.

[15] Sanjay Chouhan, Debendra Kumar Panda, Vivek Singh Kushwah, Sarthak Singhal, Spider-shaped fractal MIMO antenna for WLAN/WiMAX/Wi-Fi/Bluetooth/C-band applications, AEU - International Journal of Electronics and Communications, Volume 110, 152871, 2019.

[16] S. Shankar and D. K. Upadhyay, "A Compact Maple Leaf-shaped Frequency Reconfigurable Antenna For 5G NR, LTE, and ISM Band Applications," 2023 International Conference on Next Generation Electronics (NEleX), Vellore, India, 2023, pp. 1-6,

[17] A. A. Nikam and R. Patil, "A Honeycomb-Structured Fractal Multiband Antenna for Vehicle Communication," 2023 IEEE 3rd International Conference on Applied Electromagnetics, Signal Processing, & Communication (AESPC), Bhubaneswar, India, 2023, pp. 1-3.

[18] Sandeep Singh Sran & Jagtar Singh Sivia (2021) PSO and IFS Techniques for the design of wearable hybrid fractal antenna, International Journal of Electronics, 108:12, 2039-2057.

[19] Rania Hamdy Elabd, and Ahmed Jamal Abdullah Al-Gburi, "Design and Optimization of a Circular Ring-Shaped UWB Fractal Antenna for Wireless Multi-Band Applications Using Particle Swarm Optimization," Progress In Electromagnetics Research B, Vol. 106, 101-112, 2024.

[20] Choudhury1, B., Bisoyi, S., Jha, R.M. (2012). Emerging trends in soft computing techniques for metamaterial design and optimization. Computers, Materials & Continua, 31(3), 201-228.

[21] Kumar, E.K. and Panda, D.C. (2011). Design of Micro strip patch antenna using knowledge based soft computing techniques. International Journal of Information Technology & Management, 1(1), 1-6.

[22] Ashwini Kumar, Amar Partap Singh Pharwaha (2018). On the Design of 2×2 Element Fractal Antenna Array using Dragonfly Optimization. International Journal of Computer Applications. 179, 33, 27-34.

[23] Sushil Kakkar, Shweta Rani & A. P. Singh (2021): Triple Band Notch Microstrip Patch Antenna with Fractal Defected Ground Structure, IETE Journal of Research, 1-13.

[24] Sushil Kakkar, T. S. Kamal & A. P. Singh (2018): On the Design and Analysis of I-Shaped Fractal Antenna for Emergency Management, IETE Journal of Research, 1-10.

[25] Sushil Kakkar & Shweta Rani (2013) A novel antenna design with fractal-shaped DGS using PSO for emergency management, International Journal of Electronics Letters, 1:3, 108-117.